Coupled-System Stability of Flexible-Object Impedance Control

David W. Meer* Stephen M. Rock†
Aerospace Robotics Laboratory
Stanford University, Durand Building, Room 250
Stanford, California, 94305-4035

Abstract

This paper examines the stability of the flexible-object impedance controller when coupled to an arbitrary passive environment. A simple representative system is developed to study the problem based on phenomena observed in a more complex, experimental system. Analysis of this representative system leads to several conclusions regarding factors that limit the achievable impedances of a multi-arm system grasping a common object. The filtering of the external force signals and the effective mass contributed by the manipulators prove to be two of the important factors. Some general guidelines are developed for the successful application of flexible-object impedance control to insure coupled-system stability. These guidelines are applied to both the representative and experimental systems and verified.

1 Introduction

The advantages of using multiple manipulators include increased payload capability, improved dexterity with larger objects, and expanded functionality. Most previous research, however, focused on developing control strategies for multiple robotic arms manipulating a single, rigid body. Various potential robotic applications, from the assembly of spring-loaded parts in a manufacturing environment to the servicing of satellite solar arrays in orbit, will involve the manipulation of flexible objects by multiple robotic arms.

Object impedance control (OIC) was developed as an object-based control policy for multiple robotic arms manipulating a rigid object [11]. This work extended Hogan's impedance control concept, which attempts to regulate the relationship between the position and force at the endpoint of a single manipulator [4], to a multi-manipulator system. Recent work developed flexible-object impedance control, an extension of OIC to a class of flexible objects, and experimentally verified it [7]. Both of these controllers attempt to make the physical system behave like a reference model by cancelling the actual dynamics using a combination of feedback and feedforward control. These controllers use a reference model that specifies a programmable impedance between the object and the environment. While some mention has been made of the limitations on achievable reference model dynamics due to actuator bandwidth, no comprehensive study has been performed. This paper presents the results of an initial study designed to address that issue.

While a number of tools exist for analyzing the performance and stability of servo-controlled dynamic systems, tools for the analysis of the behavior of a controlled system coupled to the environment are less prevalent. Certainly, for a well-known environment, a model of the environment can be explicitly incorporated into the system model and the stability and performance of the system can be analyzed using conventional methods [2, 13].

This research draws on the results of another approach, taken by Fasse and Colgate, that provides a general method of analyzing the stability of closed-loop systems coupled to passive environments. [3, 1]. Colgate's research showed that a LTI n-port plant will be stable when coupled to an arbitrary passive environment iff it has the driving point impedance of a passive system [1].

A physical location where the system exchanges energy with the environment is a port. Generally, two variables, such as torque and angular velocity, whose product defines the power flow into the system at that location, characterize a port. Using bond-graph terminology, the power variables fall into two classes: efforts and flows [9]. An impedance, or a driving-point impedance, refers to the dynamic relationship between power variables at a port; more specifically, a driving-point impedance maps a flow input to an effort output. Conversely, an admittance maps an effort input to a flow output.

This analysis employs two methods of testing if a controlled system exhibits the driving point impedance of a passive system, both drawn directly from Colgate [1].

1. For MIMO systems, a passive system satisfies the requirement that $Z(jw)+Z^H(jw)$ is a non-negative definite Hermitian, where Z represents the admittance matrix of the system. Any of a number of characteristics of positive semidefinite matrices can be used to test $Z(jw) + Z^H(jw)$, including testing for non-negative eigenvalues [12].

2. For passive SISO systems, the Nyquist plot of $Z(s)$ will remain within the closed right half plane(RHP).

*Ph.D., Dept. of Mechanical Engineering.
†Assoc. Prof., Dept. of Aeronautics & Astronautics.

Consequently, the phase of the admittance of a passive SISO system must lie between -90° and 90°.

This paper applies the second test to a simple representative system to develop an understanding of the important factors affecting the coupled stability of a system under flexible-object impedance control. Based on this analysis, some general guidelines for successful application of flexible-object impedance control are derived. These guidelines are used to develop a solution and extend that solution to the experimental system. Further analysis and experimental results verify the validity of the solution.

2 Experimental System

The experimental facility, shown in Figure 1, consists of a pair of two-link manipulators in the SCARA configuration fixed to a granite surface plate, the flexible object, a fixture for the flexible object, the real-time control computer system, an overhead vision system, and a Sun workstation. The flexible object features a unique six-bar mechanism that provides a single flexible degree of freedom. More

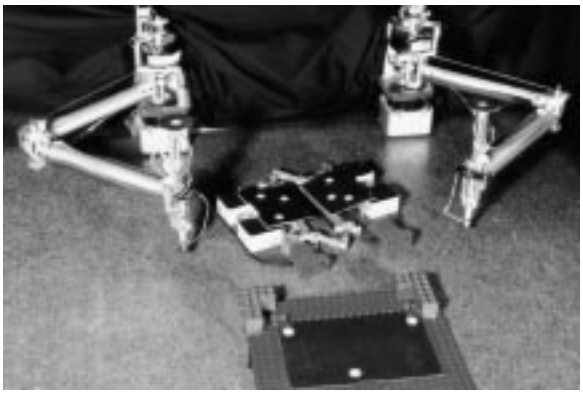

Figure 1: **Experimental Dual-Arm Hardware**

The dual arm system can perform planar motions. The object manipulated by the system floats on a cushion of air.

detailed descriptions of the manipulators, real-time vision system, and computers are contained in [10] while [6] describes the flexible object in greater detail.

3 Flexible-Object Impedance Control

Figure 2 presents a block diagram of the flexible-object impedance controller implemented on this system. This controller essentially linearizes the system using nonlinear feedback and attempts to make each degree of freedom of the object react to external forces with a programmable impedance. For a more detailed discussion of the flexible-object impedance controller, see [7]. Note that arm controllers get both desired force and desired acceleration as input from the flexible-object impedance controller. The desired acceleration allows each arm's computed-torque controller to compensate for the dynamic properties of the manipulator, including the inertia of the arm. Also note that the system has no direct measurement of the external forces acting on the object. It uses a measure of the forces applied to the object by the arms and the equations of motion of the object to estimate these external forces.

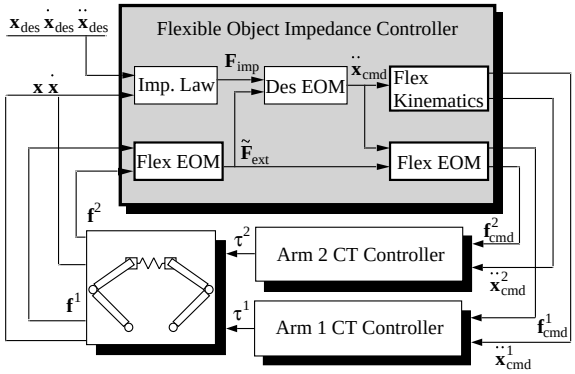

Figure 2: **Block Diagram**

The flexible-object impedance controller incorporates full kinematic and dynamic models of the flexible object.

One of the benefits of flexible-object impedance control is the ability to perform both free-space motions and contact tasks without switching control modes. Applying this control design method without considering the objective of the controller or the coupled-system stability, however, can lead to problems. Figure 3 shows the results of such a problem. In this experiment, the system is slewing the flexible object when it encounters an very rigid object in the environment. As the plot shows, this results in an unstable chattering of the flexible degree of freedom. These results motivate the introduction of a representative system to analyze the stability of the experimental system when coupled to arbitrary passive environments.

4 Representative System

For the purpose of this stability analysis, a simple mass with a single degree of freedom will serve as the representative system, since it shares certain important characteristics with the experimental system. The SISO criterion will be used to test for stability when coupled to passive environments.

4.1 System Equations

Figure 4 depicts the representative system. Following the standard impedance control derivation, the desired behavior of the system is given by:

$$m_d\ddot{x} + b_d\dot{x} + k_d x = f_{ext} \quad (1)$$

Figure 3: **Stability Problems**

Attempting to apply flexible-object impedance control without considering the stability of the system when interacting with the environment can lead to instability. During a contact experiment, such a controller could cause the object to chatter against a stiff environment.

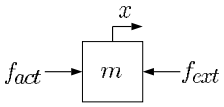

Figure 4: **Representative System Schematic**

The representative system used to examine some of the stability issues when applying object impedance control to real systems consists of a mass acted upon by two forces: an external force from the environment and the actuator force.

where m_d, b_d, and k_d represent the desired mass, damping, and stiffness of the system and f_{ext} represents the external force acting on the object. The actual equations of motion are:

$$m\ddot{x} = f_{ext} + f_{act} \tag{2}$$

where f_{act} is the actuator force. Applying the flexible-object impedance control design procedure to this system produces the following equations for $\ddot{x}_{cmd}$ and f_{act}, the commanded acceleration and actuator force required for the system to respond according to Equation 1:

$$\ddot{x}_{cmd} = \frac{\tilde{f}_{ext} - b_d\dot{x} - k_d x}{m_d} \tag{3}$$

$$f_{act} = \frac{m}{m_d}(-b_d\dot{x} - k_d x) + (\frac{m}{m_d} - 1)\tilde{f}_{ext} \tag{4}$$

where $\tilde{f}_{ext}$ represents the controller's estimate of the external force acting on the object, since no direct measurement of that force is available. Recall that the controller tries to make the system respond to f_{ext} with the programmable impedance specified in Equation 1.

If the desired mass of the reference model, henceforth referred to as the desired mass, equals the actual mass of the system, $\tilde{f}_{ext}$ has no effect on f_{act}. If the desired mass differs from the actual mass, however, when the controller senses an external force, it must instantaneously apply a force, either counteracting or reinforcing the sensed external force. Several justifications can be made for attempting to change the apparent mass of the system, including reducing impact forces, decoupling inherently coupled mass matrices, and implementing a pseudo remote center of compliance (RCC) to aid in assembly operations.

4.2 Coupled-System Stability Analysis

If the desired mass does not equal the actual mass, the estimated external force will affect the commanded control torques sent to the manipulators. With an exact measure of the external force, any impedance relationship is achievable, neglecting actuator limitations. Since the force signals in the experimental system undergo low-pass filtering to reduce the noise from the strain-gage measurements:

$$\tilde{f}_{ext} = \frac{\omega_n^2}{s^2 + 2\zeta\omega_n + \omega_n^2} f_{ext} \tag{5}$$

The estimate of the external force runs through a second order low pass filter with break frequency ω_n and damping ζ. Solving for the admittance of the system produces the following equation:

$$A(s) = \frac{\dot{x}}{f_{ext}} = \frac{\frac{s^3 + 2\zeta\omega_n s^2}{m} + \frac{\omega_n^2 s}{m_d}}{(s^2 + 2\zeta\omega_n s + \omega_n^2)(s^2 + \frac{b_d}{m_d}s + \frac{k_d}{m_d})} \tag{6}$$

This admittance will have a phase that moves from +90° at low frequencies to -90° at high frequencies. Depending upon ω_n^2 and $\frac{k_d}{m_d}$, however, the phase could pass outside these boundaries for regions of the frequency domain.

To examine the effects of varying the desired mass from the actual mass, either or both could be changed. Since changing the desired mass would also require changing the damping and stiffness coefficients in Equation 1 to maintain the same controlled bandwidth, the actual mass was varied.

Figure 5 shows the Bode and Nyquist plots for values of the actual mass corresponding to twice and four times the desired mass. The numbers used for the various system parameters are normalized from the values for a single degree of freedom of the flexible object. In this case $m_d = 1$ kg, $k_d = 60$ N/m, $b_d = 15.49$ N − s/m, $\omega_n = 987$ rad/s^2, and $\zeta = 0.75$. Plots for the target admittance are included for reference. This plot shows the general trend when the controller attempts to decrease the apparent mass of the system. Note that the phases of the admittances for both of the systems with $\frac{m_d}{m} < 1$ drop below -90°. Thus, the Nyquist plots for both these systems have loops that enter the left half plane, indicating instability when coupled to stiff environments.

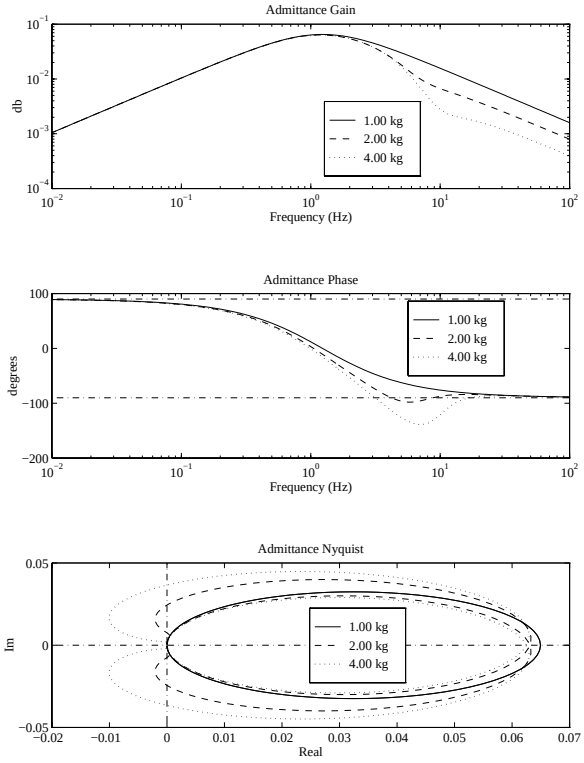

Figure 5: **Effects of Decreasing Mass**

Attempts to decrease the mass of the system can lead to instability. The Bode plots of the admittance of the system for $\frac{m_d}{m}$ ratios of 1, $\frac{1}{2}$, and $\frac{1}{4}$ show that, for both systems with $m_d < m$, the phases pass below the -90° stability boundary. Consequently, the Nyquist plots for these cases pass into the left half plane, indicating instability.

Figure 6 shows a root locus for the representative system coupled to an environment consisting only of a linear spring as the stiffness coefficient of the spring varies. For this case, the actual mass is 2 kg. The locus shows that a pair of roots leave the left half plane when the environmental stiffness is about 1075 N/m and return when the environmental stiffness is approximately 7375 N/m. Thus, as predicted by the coupled-system stability analysis, the system exhibits conditional stability: it exhibits unstable behavior when coupled to environments with a range of stiffnesses.

In summary, for the simple representative system, the coupled stability criterion has shown that attempting to decrease the apparent mass can lead to instability when the system interacts with stiff environments.

4.3 Effects of Actuator Dynamics

The previous analysis assumed that the actuator could provide a specifiable force acting on the object. In most

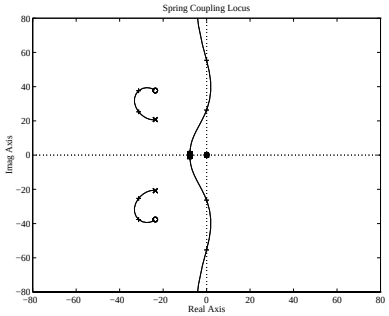

Figure 6: **Root Locus for Coupling to Spring Environment**

Modeling the environment as a linear spring and plotting a locus versus the environmental stiffness shows that the closed-loop poles of the representative system under impedance control with $\frac{m_d}{m} = \frac{1}{2}$ can pass into the right half plane. The +'s represent the points where the roots enter and leave the right half plane, at $k_{env} = 1075$ N/m and $k_{env} = 7375$ N/m, respectively.

real mechanical systems, including the experimental system used for this work, the actuators are not simple force sources: they have dynamics of their own. Recognizing this, the flexible-object impedance controller passes the desired arm endpoint accelerations as well as the desired endpoint forces to the individual arm controllers. This enables the arm controllers to compensate for the arm dynamics. In the case of the highly idealized, direct-drive arms used in this research, the inertia of the manipulators is the principal dynamic effect that must be taken into account.

To understand how the actuator inertia affects the stability analysis, an actuator model is added to the representative system, as shown in Figure 7. A simple mass, m_{act},

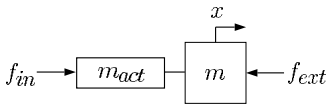

Figure 7: **Addition of Actuator Inertia**

This schematic shows the addition of actuator dynamics, represented by the additional mass, m_{act}, to the representative system.

rigidly coupled to the object models the actuator dynamics. The calculated input force, f_{in}, acts on the actuator mass. Equation 4 still produces the commanded actuator force, f_{act}, but now the controller also attempts to compensate for the actuator dynamics:

$$f_{in} = f_{act} + m_{act}\ddot{x}_{cmd} \tag{7}$$

Substituting the results of Equations 4 and 3 and simplifying produces the expression:

$$f_{in} = \frac{m_{act}+m}{m_d}\left(-b_d\dot{x} - k_d x\right) + \left(\frac{m_{act}+m}{m_d} - 1\right)\tilde{f}_{ext} \tag{8}$$

This equation shows that the mass ratio that determines the stability of the system is actually $\frac{m_{act}+m}{m_d}$ not simply $\frac{m}{m_d}$, so the actuator mass plays an important role in determining the coupled-system stability.

In the actual experimental system, this factor becomes even more important, since the object is grasped by a pair of manipulators. In fact, flexible-object impedance control is derived for an arbitrary number of manipulators grasping the object. In that case, the sum of the effective inertias of the manipulators may dominate the total inertia of the system.

The fact that the effective inertia of an object grasped by multiple manipulators includes the inertia of the manipulators is not a new result. Khatib's work on extending the operational space technique for control of systems with multiple manipulators grasping a common object demonstrated that the effective inertia of an object grasped by a number of arms in parallel was the sum of the inertias taken about a single operational point [5]. The object impedance control technique, however, which draws on the work of Nakamura [8], separates the controller into 2 distinct parts: an object controller that generates desired forces and accelerations for the arm endpoints and the arm controllers which calculate the necessary command inputs for each arm. Looking at the controller from this perspective, it is tempting to treat the arms as "virtual" actuators and ignore their contributions to the dynamic behavior of the grasped object.

Calculating the values of the diagonal elements of the mass matrix for the system (including the arms and the object) throughout the workspace of the arms, since the values vary with configuration, produced values of $\frac{m_{total}}{m_{object}}$ ranging from 1.29 to 8.22. In this calculation, m_{total} represents the total effective mass of the system in a single degree of freedom and m_{object} is the contribution from the flexible object. Since the desired mass parameters were chosen to approximately match the diagonal elements of the object's mass matrix, $\frac{m_{total}}{m_{object}} \simeq \frac{m_{act}+m}{m_d}$. As the analysis of the representative system shows, even an attempt to decrease the apparent mass by a factor of 2 can result in stability problems.

4.4 Solution Alternatives

Changing the desired mass parameters to reflect more closely the mass of the actual system would solve the stability problems. As noted previously, however, these inertia parameters vary considerably across the workspace of the dual-armed system. Also, to maintain a consistent bandwidth of about 1.5 Hz, an increase of 400% in the mass of the virtual object would also require a similar increase in the stiffness term in the impedance law, resulting in a very stiff system with relatively large forces generated by small errors.

The force filter coefficients are another set of parameters that could be changed to affect the coupled-system stability. Equation 9 presents the admittance of the representative system with actuator dynamics included.

$$A(s) = \frac{\frac{1}{m_{act}+m}(s^3 + 2\zeta\omega_n s^2 + \frac{m_{act}+m}{m_d}\omega_n^2 s)}{(s^2 + 2\zeta\omega_n s + \omega_n^2)(s^2 + \frac{b_d}{m_d}s + \frac{k_d}{m_d})} \qquad (9)$$

Looking at this equation, the filter introduces a pair of poles and a pair of zeros. When $\frac{m_d}{m_{act}+m} < 1$, the filter zeros enter at a higher frequency than the filter poles, introducing phase lag. Consequently, raising the force filter frequency will only serve to raise the range of stiffnesses that lead to instability. Lowering the force filter frequency, on the other hand, should improve the coupled-system stability by moving the frequency at which the filter effects appear below the range where the phase of the desired admittance is close to -90°.

When attempting to increase the effective mass of the system ($\frac{m_d}{m_{act}+m} > 1$), however, the filter zeros occur at a lower frequency than the filter poles, introducing some phase lead. In this case, the filter cutoff frequency should be above the frequency determined by the bandwidth of the reference model ($\frac{k_d}{m_d}$) to insure coupled-system stability. This will keep the phase lead from the force filter out of the region where the phase of the reference admittance approaches +90°.

So, two choices are available to solve the instability problems in this representative system: lower the force filter frequency or increase the desired mass properties of the controller above the maximum values calculated for the system. For this experimental system, the option that lowered the force filter frequency was chosen.

Figure 8 shows how lowering the force filter frequency from 5 Hz to 1.5 Hz changes the coupled-system stability. Now the effective mass of the system can be reduced by a factor of 3.45 without resulting in instability when coupled to a passive environment.

Even with this improvement, it is not enough to cover the range of variations in the effective inertia seen when moving the flexible object throughout the workspace. This analysis only considered the diagonal terms of the mass matrices, however, not the fully coupled matrix that occurs in the real experimental system.

5 Extension to Experimental System

To verify that decreasing the force filter cutoff frequency also works on the full nonlinear equations of motion of the experimental system, a more complex analysis was performed.

To check the coupled-system stability of the experimental system, the system equations of motion (both the object and the manipulators) were linearized about over 4000 points in the workspace. At each of these points, the eigenvalues of the admittance matrix were calculated across a frequency range of 0.0001 rad/s to 10000 rad/s. This process returned two sets of data: the minimum eigenvalue at each frequency, regardless of position, and the minimum eigenvalue at each x, y location in the workspace, regardless of frequency or θ position. The upper plot presents the

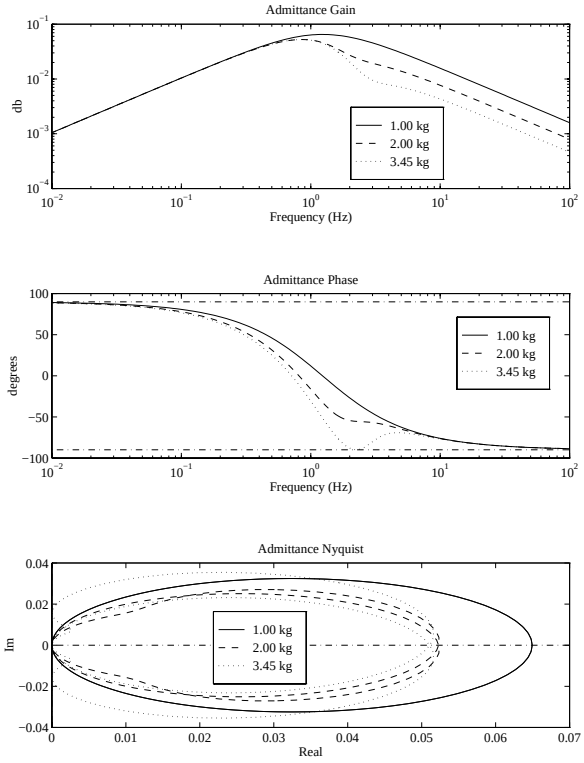

Figure 8: **Force-Filter Frequency Effects on Coupled-System Stability**

Lowering the force-filter cutoff frequency improves the coupled-system stability of the representative system. Now the controller can interact stably with any passive environment with a mass ratio of $\frac{m_d}{m+m_{act}} = \frac{1}{3.45}$.

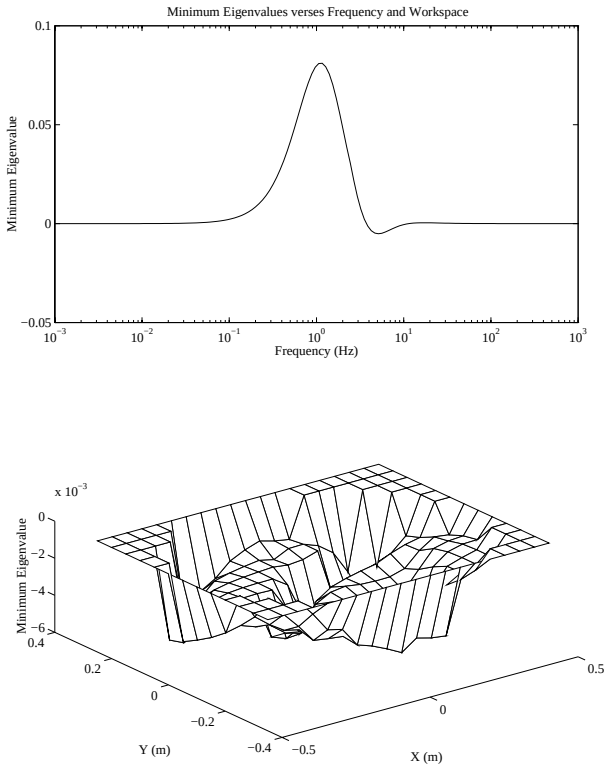

Figure 9: **5 Hz Force Filter**

As observed experimentally, the system with a 5 Hz force filter on the estimated external force measurements will exhibit instability when interacting with certain stiff environments.

minimum eigenvalue as a function of frequency while the bottom plot shows the minimum eigenvalue of the admittance matrix as a function of x, y position. In the lower plot, those values of the workspace that were unreachable have a minimum value of zero.

Figure 9 demonstrates that, with the break frequency for the force filter at 5 Hz, as originally attempted, the system exhibits coupled instability. The lowest eigenvalue at any reachable point in the workspace is negative in this case. Thus, at any point in the workspace, the system would be unstable if coupled to an environment with a certain stiffness.

Figure 10, on the other hand, demonstrates that lowering the force filter cutoff frequency to 1.5 Hz solves the coupled-system stability problem. Notice that all of the minimum eigenvalues are positive. Thus, the system should perform stably when coupled to an arbitrary passive environment.

Finally, Figure 11 compares the results of the contact experiment for the two force filter cutoff frequencies. Clearly, the controller can now bring the object stably into contact with a very stiff environment.

6 Conclusions

This paper developed some general guidelines for successfully applying flexible-object impedance control to a system composed of multiple manipulators grasping a flexible object to insure stability of the system when coupled to arbitrary passive environments. The interaction between filtering on the estimated external force and the desired impedance behavior of the object can lead to instability. This conflict can be resolved by altering either the filter parameters or the desired impedance parameters. These guidelines were developed through analysis of a simple linear system and then applied to the experimental system and verified, both analytically and experimentally.

This paper also demonstrated that the inertia of the manipulators grasping the object has a significant affect on the coupled-system stability of the system and must be considered when selecting the desired impedance parameters.

Acknowledgements

The work reported in this paper was initially funded by a

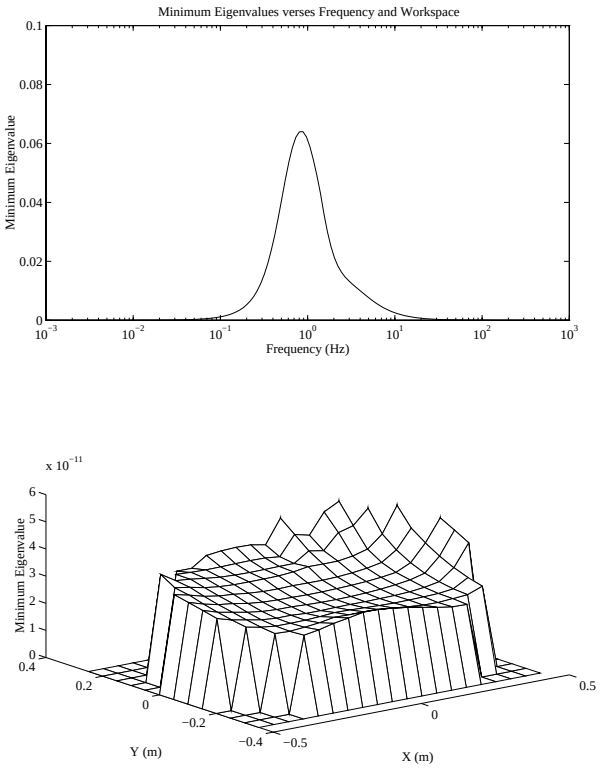

Figure 10: **1.5 Hz Force Filter**

Lowering the force filter cutoff frequency to 1.5 Hz produces a system that interacts stably with any passive environment in the experimental system, just as it did in the representative system.

grant from the Stanford Integrated Manufacturing Association (SIMA) and continued under NASA contract NCC-2-333. The authors gratefully acknowledge the assistance and support of the students and staff of the Aerospace Robotics Laboratory.

References

[1] James Edward Colgate, *The Control of Dynamically Interacting Systems*, PhD thesis, Massachusetts Institute of Technology, Department of Mechanical Engineering, August 1988.

[2] Steven D. Eppinger and Warren P. Seering, "On Dynamic Models of Robot Force Control," *Proceedings of the IEEE International Conference on Robotics and Automation*, San Francisco, CA, April 1986, pages 29–34.

[3] E. D. Fasse, "Stability Robustness of Impedance Conrtolled Manipulators Coupled to Passive Environments," Master's thesis, Massachusetts Institute of Technology, Department of Mechanical Engineering, June 1987.

[4] Neville Hogan, "Impedance Control: An Approach to Manipulation," *Transactions of the ASME, Journal of Dynamic Systems, Measurement, and Control*, Vol. 107, March 1985, pages 1–24.

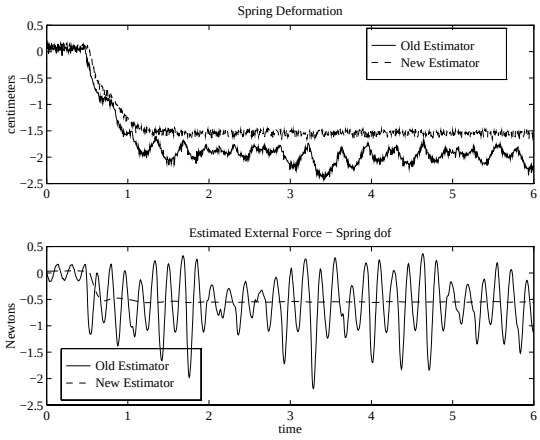

Figure 11: **Improved Estimator Results**

Changing the cutoff frequency of the filter on the external force estimator, as recommended by the coupled-system stability analysis, dramatically improves the performance of the experimental system, enabling it to stably contact a very stiff obstacle in the environment.

[5] O. Khatib, "Object Manipulation in a Multi-Effector Robot System," *Robotics Research: the Fourth International Symposium*, Santa Cruz, CA, MIT Press, 1987.

[6] David W. Meer and Stephen M. Rock, "Cooperative Manipulation of Flexible Objects: Initial Experiments", *Proceedings of the ASME Winter Annual Meeting: Dynamics of Flexible Multibody Systems: Theory and Experiment*, Anaheim, CA, November 1992, pages 1–4.

[7] David W. Meer and Stephen M. Rock, "Experiments in Object Impedance Control for Flexible Objects," *Proceedings of the IEEE International Conference on Robotics and Automation*, San Diego, CA, May 1994, pages 1222–1227.

[8] Y. Nakamura, K. Nagai, and T. Yoshikawa, "Mechanics of Coordinative Manipulation by Multiple Robotic Mechanisms," *Proceedings of the IEEE International Conference on Robotics and Automation*, Raleigh, NC, April 1987, pages 991–998.

[9] H. M. Paynter, *Analysis and Design of Engineering Systems*, M.I.T. Press, Cambridge, MA, 1961.

[10] S. Schneider, *Experiments in the Dynamic and Strategic Control of Cooperating Manipulators*, PhD thesis, Stanford University, Stanford, CA 94305, September 1989. Also published as SUDAAR 586.

[11] S. Schneider and R. H. Cannon, "Object Impedance Control for Cooperative Manipulation: Theory and Experimental Results", *IEEE Journal of Robotics and Automation*, Vol. 8, No. 3, June 1992. Paper number B90145.

[12] Gilbert Strang, *Linear Algebra and its Applications*, Harcourt Brace Jovanovich, Orlando, FL, third edition, 1988.

[13] Richard Volpe and Pradeep Khosla, "Theoretical Analysis and Experimental Verification of a Manipulator/Sensor/Environment Model for Force Control," *Proceedings of the IEEE International Conference on Systems, Man, and Cybernetics*, November 1990, pages 784–790.